Physica B 626 (2022) 413499

Contents lists available at ScienceDirect

Physica B: Physics of Condensed Matter

journal homepage: www.elsevier.com/locate/physb

The effect of charge and spin state on the Infrared spectra and hyperfine coupling constants of point defects in Silicon

Alexander Platonenko [a], Fabien Pascale [b], Khaled E. El-Kelany [c], Francesco Silvio Gentile [d,*], Roberto Dovesi [e]

[a] Institute of Solid State Physics, University of Latvia, 8 Kengaraga street, LV1063, Riga, Latvia
[b] Université de Lorraine - Nancy, CNRS, Laboratoire de Physique et Chimie Théoriques, UMR 7019, Vandoeuvre-les-Nancy, France
[c] Institute of Nanoscience and Nanotechnology, Kafrelsheikh University, 33516 Kafrelskiekh, Egypt
[d] Department of Chemical Sciences - Università degli Studi di Napoli Federico II - Complesso Universitario di Monte Sant'Angelo, Via Cintia, 21 80126 Napoli, Italy
[e] Dipartimento di Chimica, Università di Torino and NIS (Nanostructured Interfaces and Surfaces) Centre, Via P. Giuria 5, 10125 Torino, Italy

ARTICLE INFO

Keywords:
Defects
Bulk silicon
Charge state
Spin state
Geometry
IR spectra
Hyperfine coupling constants

ABSTRACT

The effect of the charge of a point defect on the infrared spectrum and the hyperfine coupling constants is discussed with reference to the VO defect in silicon. Five charge states have been considered, from +2*e* to −2*e*. Calculations are performed by using a local Gaussian type basis set and the B3LYP hybrid functional. The dominant peak in the IR spectrum increases linearly from 708 cm^{-1} (+2 charge), to 904 cm^{-1} (−2 charge). The intensity decreases from 4073 to 1727 km/mol, as a consequence of the reduced polarity of the Si-O bond. Also the hyperfine constants differ by large percentages along the series. Although limited to a single defect, the present study shows that both the IR and EPR techniques are able to discriminate the charge state of the defect, also in the cases in which more than one charge state is present in the same sample.

1. Introduction

The identification of the defects present in a crystalline compound is not an easy task. Evidences can be provided by various tools, the most common being the optical, IR, Raman and EPR spectra [1–5]. The modifications of these spectra is the information that must be analyzed for inferring the microscopic local nature of the defect. As there is no signal from IR and EPR experiments in perfect diamond or silicon bulk, whose Raman spectrum is characterized by a single [6], very intense peak, any peak appearing in the IR spectrum of the defective system, or any additional peak in the Raman spectrum, or any EPR signal, provides the evidence of the presence of the defect.

However, associating the features of the experimental IR, Raman or EPR spectra to a specific defect (chemical nature, geometry, electronic structure) is always challenging and, very often, controversial. This is all the more true when more than a single defect is present, which is the general case rather than the exception, because the features of one defect can be altered by the other. For example, when a vacancy is created, the *removed* atom must occupy an interstitial position (or another lattice position, in cases with many vacancies at short distances). So, in the best cases we have two defects, the vacancy and the interstitial atom, that in general can both generate a signal for IR, Raman, EPR. Also the evaluation of the concentration of these intrinsic defects can be challenging.

When heteroatoms are present, and their chemical nature and concentration is established, the number of different possible distributions of X atoms (say oxygen) in the various positions is huge (in principle infinite). There are however additional variables that can alter the response of the defective system to the external perturbation. Two, very important, are the charge state of the defect, and its spin state. IR and Raman experiments do not provide direct information on both, and EPR only on the latter. In the same sample, the same defect can appear in more than one charge or spin state, as is the case, for example, of *N* substitutional (N_s), that can appear in various charge states when N_s and NV^0 (a defect formed by a substitutional nitrogen atom, N_s, first neighbor of a vacancy; the zero superscript indicate that this defect is neutral) transforms to N^+ and NV^- (see References [7] and [8]).

This short manuscript is aimed to deepen the analysis of this point. In particular, for a specific point defect, VO in silicon (one vacancy with one oxygen atom filling partially the empty space) we investigated 5 charge states (+2, +1, 0, −1, −2) and three spin states (triplet, doublet, singlet).

Simulation can play an important role in clarifying the specific question of the charge and spin state, and of its influence on the IR,

* Corresponding author.
E-mail address: francesco.gentile@unina.it (F.S. Gentile).

https://doi.org/10.1016/j.physb.2021.413499
Received 26 August 2021; Received in revised form 13 October 2021; Accepted 24 October 2021
Available online 11 November 2021

Table 1
Structural and electronic parameters of the VO defects in various charge (column 1) and spin (column 2) states (s, d and t stand for singlet, doublet and triplet). q is the atomic net charge, μ is the corresponding spin quantity (both in $|e|$), d_{X-Y} are the distances, in Å. See Fig. 1 for the labels of the atoms. The two sets of neighbors, Si_1 and Si_2, and Si_3 and Si_4 (see Fig. 1) are equivalent in all but VO+ cases, as indicated in Table 3. The spin density at Si_4 for this defect is visible in Fig. 3.

Charge	Spin	q_O	μ_O	q_{Si_1}	μ_{Si_1}	q_{Si_3}	μ_{Si_3}	d_{O-Si_1}	$\angle_{Si_1-O-Si_2}$	$d_{Si_3-Si_4}$
+2	s	−0.759	0.0	+0.396	0.0	+0.228	0.0	1.750	131.7	4.511
	t	−0.722	−0.002	+0.412	+0.003	+0.141	+0.427	1.751	131.8	4.511
+1	d	−0.706	+0.009	+0.361	+0.018	+0.037	+0.674	1.733	138.0	4.260
0	s	−0.643	0.0	+0.346	0.0	+0.039	0.0	1.712	147.1	3.183
	t	−0.655	0.020	+0.361	+0.021	+0.029	+0.788	1.713	142.3	4.140
−1	d	−0.588	+0.015	+0.337	+0.005	−0.036	+0.355	1.693	152.3	3.580
−2	s	−0.547	0.0	+0.330	0.0	−0.092	0.0	1.680	159.1	3.630
	t	−0.545	−0.042	+0.267	0.168	−0.042	0.367	1.698	155.6	3.620

Raman and EPR spectra, as by input the defects can be inserted one at the time in perfect bulk, with a well defined charge state *around the defect* and a well defined spin state of the wavefunction in the unit cell.

We will then try to answer the three questions:

(a) how large is the modification of the IR spectra of these defects when their charge is changing? How large is the shift of the most dominant peak, if any, that can be used as a *fingerprint* of the defect? What about the intensity of this peak when the charge state is changing?

(b) what about the influence of the charge state on the EPR spectra?

(c) what is the influence of the spin state on the IR and Raman spectra?

A series of defects containing the vacancy V and one to four oxygen atoms per cell have recently been investigated by some of the present authors [9], and characterized through the IR spectrum. In most of the cases the Raman spectrum is dominated by the pristine silicon peak at about 533 cm^{-1} and is then not very useful for the characterization of the defect.

Five charge states have been considered for the VO defect, namely +2, +1, 0, −1 and −2. When the charge is even, then also the number of electrons in the unit cell is even. It is then possible to have singlet ($S_z = 0$), triplet ($S_z = 1$), quintet ($S_z = 2$), ...spin states. Only the first two have been considered, the other having much larger total energy. When the charge is odd (+1, −1), then a doublet ($S_z = 1/2$) or a quadruplet ($S_z = 3/2$) spin state is possible. Only the first, usually the ground state, has been considered here. In the −2 charge system, we have been able to converge the Self-Consistent Field (SCF) solution only for the singlet. The triplet and the singlet solutions for the +2 and 0 cases provide enough information on the effect of the spin state on the IR spectrum.

The paper is structured as follows. Section 2 provides a short description of the geometry, the charge and spin (when applies) density, and of the IR and EPR spectra of the defects. A few conclusions are drawn in Section 3. A Supplementary Material Section describes the main features of the method here adopted. As they are exactly the same as used in recent applications to defects in diamond [10] and silicon [11–13], they are not inserted in the main body of the manuscript, but simply proposed for ease of consultation from the reader. Here we simply remind that calculations have been performed by use of the B3LYP global hybrid functional [14,15], as implemented in the CRYSTAL17 program [16]. An *all-electron* basis set of Gaussian-type functions has been adopted; the supercell model has been used, by expanding the conventional cell containing 8 atoms by two along the three lattice parameters (64 atoms before creation of the vacancy). The calculations were spin polarized, also in the cases in which the final result is a closed shell. Atomic net charges q and atomic magnetic moments μ reported in Table 1 have been computed through a Mulliken analysis.

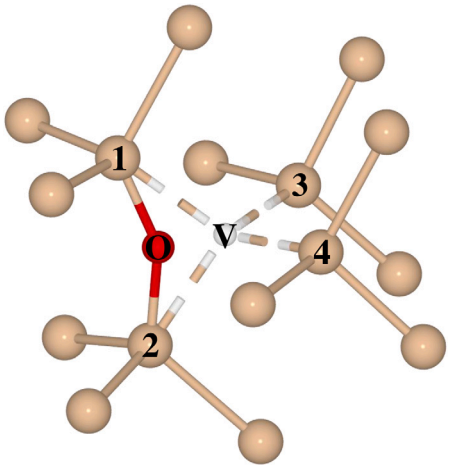

Fig. 1. Schematic representation of the VO defect in silicon, with the labels of the atoms as used in the tables.

2. Results

2.1. Equilibrium geometry

We start the analysis of the geometry and of the charge and spin density from the neutral case, both singlet s and triplet t. The results of the Mulliken analysis are shown in Table 1. For *s*, the atomic net charge q of O is $-0.64|e|$, nearly exactly compensated by the net charges of the two silicon atoms Si_1 and Si_2 = $+0.35|e|$. The Si_1-O distance is 1.71 Å and the Si-O-Si angle is 147°. In the *t* state the numbers are very similar: the Si-O-Si angle is however 142°; the two unpaired electrons are localized to a large amount on the *opposite* Si atoms (Si_3 and Si_4, see Fig. 1), with μ= +0.79 $|e|$. Due to the Pauli repulsion between the two unpaired electrons, the Si_3-Si_4 distance increases by 30%, from 3.18 to 4.14 Å. We can now look at the variations along the columns in Table 1, when going from the +2 to the −2 charge state. The charge on oxygen reduces from −0.72 to −0.55 $|e|$, and the one on Si_1 and Si_2 from +0.41 $|e|$ to $+0.27|e|$, with a large reduction of the polarity of the bond, and a consequent reduction of the IR intensity, as will be documented in Table 2. In going from the +2 to the −2 charge state, the Si-O bonds reduces from 1.75 to 1.70 Å, and the Si_2-O-Si_1 angle increases from 132° to 156°. The change in the net charges of Si_3 and Si_4 is much larger; they drop from +0.39 to −0.09 $|e|$, and then change sign. The net charges of the singlet and triplet solutions are extremely similar.

The spin density is localized to a large amount on Si_3 and Si_4, as documented by Fig. 3 and by the μ values of Table 1, with the exception of VO^+; in this case the uncoupled electron is trapped mainly on Si_3 only. In the extreme charge cases (−2 and +2) the spin density is more delocalized than when the charge in the unit cell is smaller.

Table 2
Wavenumbers (in cm^{-1} and black) and intensities (in km/mol and red) of the most intense peaks of the VO defects in various charge (column 1) and spin (column 2) states (s, d and t stand for singlet, doublet and triplet).

Charge	Spin	Wavenumber and intensity					
+2	s	708	4073	556	503	267	421
	t	718	4083	555	476	268–276	600
+1	d	765	3294	556	250	261–273	150
0	s	819	2874	550–536	196	406–411	90
	t	811	2817	563	108	248–271	120
−1	d	867	2260	523–558	115	400–420	200
−2	s	904	1727	560	10	490–494	40

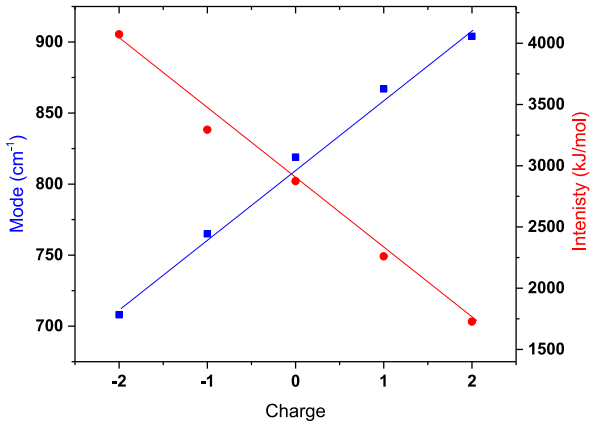

Fig. 2. Vibrational wavenumbers (blue, left scale) and IR intensities (red, right scale) as a function of the charge state. The continuous curves are obtained with a linear fit. Squares and dots are the calculated points (see also Table 2). (For interpretation of the references to color in this figure legend, the reader is referred to the web version of this article.)

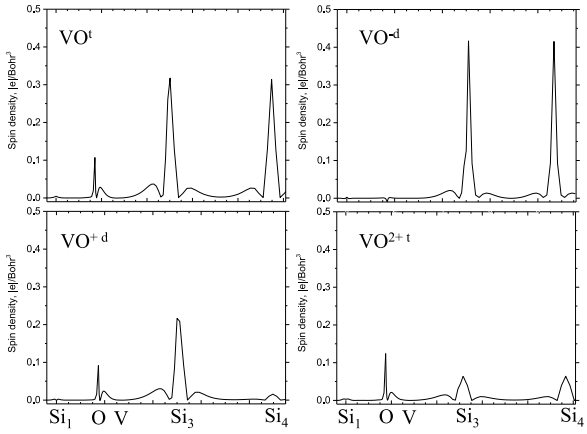

Fig. 3. Spin density along the Si_1-O-V-Si_3-Si_4 path.

2.2. Vibrational spectra

For symmetry reasons, the IR spectrum of pristine silicon is featureless, while the Raman spectrum exhibits a single absorption mode at 521 cm^{-1} (see Ref. [6]). So the entire IR spectra of defective systems can be attributed to the presence of defects, as can all Raman peaks other than the one at 521 cm^{-1}. The calculated Raman peak with the present functional and basis set is at 533 cm^{-1}, 12 cm^{-1} above the experiment.

The modes to which O contributes appear well above the calculated pristine silicon peak at 533 cm^{-1}, as oxygen is lighter than silicon (16.0 vs 28.1 a.u.). The O-Si bonds are polar (typical electronegativity values are 1.8 for Si and 3.4 for O), so that the IR *defect peaks* are very intense and dominate the spectrum.

The spectrum in all cases span the 100–530 cm^{-1} interval, with a couple of modes around 550–560 cm^{-1} and the dominant peak above 700 cm^{-1}, as Table 2 shows. The three most intense peaks for the various cases are reported, with their intensity in km/mol (red columns). A few comments:

- in each case, the most intense peak is at the highest wavenumber, and corresponds to a Si-O stretching.
- The wavenumber increases (nearly) linearly when the charge of the defect changes from +2 to −2, as Fig. 2 shows (note that the fit is linear).
- The intensity I decreases *linearly* from nearly 4000 km/mol (for the +2 case) to 1700 km/mol (−2 case), as Fig. 2 shows.
- The second most intense peak for the +2 charge state is at 556 cm^{-1}, with I = 503 km/mol. The wavenumbers remain essentially constant in the full charge interval; the intensity, however, drops from 500 (+2) to 100 (0) to 10 (−2) kJ/mol, as was the case for the peaks above 700 cm^{-1}.
- The difference in frequency between the triplet and singlet spin states for the dominant peak is relatively modest: +10 and −8 cm^{-1} for the +2 and 0 charge cases. The intensity is nearly unchanged (+0.2% and −2%, respectively).
- The third peak is well within the perfect silicon vibrational manifold, and is not easily characterized, nor its dependence on the charge state presents systematic features (see Fig. 4).

2.3. The hyperfine coupling constants

In Fig. 3 the spin density profiles along the oxygen atom and its four first neighbors Si_1, Si_2, Si_3 and Si_4 (see Fig. 3) are shown. The spin density at the atomic position and the four parameters characterizing the hyperfine interaction, namely the Fermi contact A_{iso}, and the three diagonal components of the hyperfine coupling tensor B are shown in Table 3. It should be noticed that Si_1 is equivalent to Si_2, and Si_3 to Si_4 in all cases, the exception being VO^+. In the last line of the Table also some experimental data, nearly 50 years old, referring to O and attributed to VO^-, are reported.

We remind that we are trying to answer to the following question: are the hyperfine constants such to permit to distinguish between various charged states of a given defect, when the latter is for some reason undefined, or the defect appears in the sample in two charge states?

Looking at the A_{iso} data, that are proportional to the spin density shown in Fig. 3, we notice:

a. On oxygen, A_{iso} is positive in 4 out of 5 cases, with values that differ in general by about 15 MHz from case to case, with the exception of VO^0 and VO^+. These two cases have however a different spin multiplicity (triplet and doublet), so that EPR can easily distinguish one from the other.

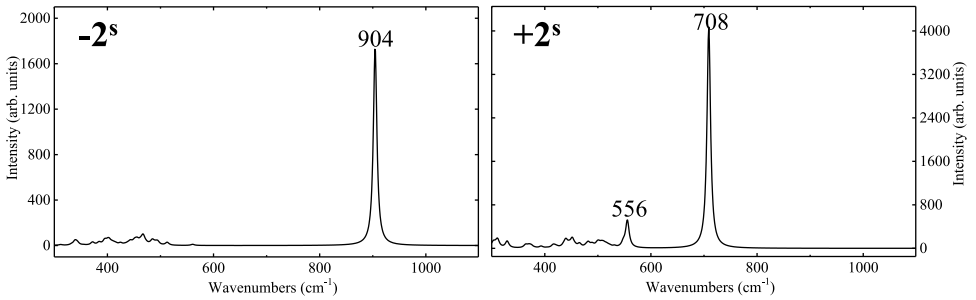

Fig. 4. Calculated IR spectra of the singlet state of the +2 and −2 charge cases.

Table 3
Fermi contact and hyperfine coupling tensor components (both in MHz) of the VO defects in various charged states. In the first column also the spin density ρ ($|e|/Bohr^3$) at the nuclear position is reported. B tensor components are sorted so that $|B_1| > |B_2| > |B_3|$. The point symmetry in the five cases is, from top to bottom, C_{2v}, C_{2v}, C_s, C_{2v} and C_s. Si_3 and Si_4 are equivalent in all but VO^+ cases, as indicated in the "Atom" column.

		Atom	ρ	A_{iso}	B_1	B_2	B_3
Triplets	VO^{2+}	O_1	0.0298	−18.11	−1.36	0.97	0.39
		Si_3 (Si_4)	0.05875	−52.21	−19.97	10.35	9.62
	VO^0	O_1	0.107	−64.57	7.79	−5.24	−2.55
		Si_3 (Si_4)	0.314	−279.11	−153.77	76.89	76.88
	VO^{2-}	O_1	0.1215	−36.81	−3.90	2.11	1.78
		Si_3 (Si_4)	0.440	−195.62	−67.91	33.08	34.83
Doublets	VO^+	O_1	0.0981	−59.47	−8.33	4.31	4.03
		Si_3	0.2214	−196.77	−130.98	65.86	65.12
	VO^-	O_1	−0.0089	5.45	−5.16	3.28	1.88
		Si_3 (Si_4)	0.4151	−368.90	−67.13	32.30	34.83
	VO^- EXP [17]	Si (x2)	–	−410.3	−48.4	24.2	24.2

b. The largest A_{iso} value is on Si_3 (and obviously Si_4 when they are equivalent). The differences among the three triplets are larger than 100 MHz. The values of the two doublets differ by much more than 100 MHz.
c. As regards the B values of oxygen (we look at B1, the largest component in absolute value; remember that the tensor is traceless, and then $B_1 = B_2 + B_3$), for the doublets they differ by more than 3 MHz (that is nearly 40%), and for the triplets the differences are similar, with two negative (VO^{2+} and VO^{2-}) and one positive (VO^0) values, spanning overall nearly 12 MHz.
d. For the Si_3 triplets, the B_1 values are 20, 154 and 68 MHz, easily distinguishable. For the Si_3 doublets the situation is similar, with very different values for VO^+ and VO^-, 131 and 67 MHz.
e. We have been able to find only a single set of experimental data, attributed to Si in VO^-. The A_{iso} value reported by Watkins and Corbett is 410 MHz; it compares reasonably well (+10%) with our calculated values for Si_3. The difference for the B_1 component is larger, nearly 40%. In spite of these relatively large differences, the possible attribution of the experimental spectrum to the other doublet state, VO^+, can be excluded, as the differences would be much larger, both for A_{iso} and B_1.

In summary, taking into account that the triplet and doublet EPR spectra are quite different, and then the defect charge effect must be discussed within the two families, we can conclude that, at least for this defect, in the cases in which the charge state is unknown, or more than a charge defect state is present in different zones of the defective system, hyperfine constants should be such to allow a clear identification of the charge value.

3. Conclusions

The effect of the charge of a local defect on the IR spectrum (wavenumbers and intensities) and on the constants characterizing the hyperfine coupling constants is explored by considering five charge states, namely +2, +1, 0, −1, −2, of the VO defect in silicon (a vacancy filled by an oxygen atom); the IR dominant peak increases, linearly, by about 200 cm^{-1}, and the intensity decreases from 4100 to 1700 km/mol in going from the +2 to the −2 solution, so that all the charge states are well separated in wavenumber and intensity. The same is true for the three triplet (charge +2, 0, −2) and two doublet (+1, −1) states, whose A_{iso} and B values vary by large percentages from one charge state to another. We can then suppose that in general IR and EPR techniques should be able to produce spectra quite different from charge state to charge state, at least for some of the features of the respective spectra.

CRediT authorship contribution statement

Alexander Platonenko: Conceptualization, Methodology, Formal analysis, Writing – original draft. **Fabien Pascale:** Software, Data curation, Writing – review & editing. **Khaled E. El-Kelany:** Writing – review & editing. **Francesco Silvio Gentile:** Conceptualization, Methodology, Data curation, Visualization. **Roberto Dovesi:** Project administration, Conceptualization, Writing – original draft, Supervision.

Declaration of competing interest

The authors declare that they have no known competing financial interests or personal relationships that could have appeared to influence the work reported in this paper.

Data availability

The data that supports the findings of this study are available within the article and references therein.

Acknowledgments

Calculations were performed using Latvian Super Cluster (LASC), located at the Center of Excellence at the Institute of Solid State Physics, University of Latvia, which has received funding from European Union's Horizon 2020 Framework Programme H2020-WIDESPREAD-01-2016-2017-TeamingPhase2 under grant agreement No. 739508, project CAMART^2

Appendix A. Supplementary data

Supplementary material related to this article can be found online at https://doi.org/10.1016/j.physb.2021.413499.

References

[1] A. Mainwood, Modelling of interstitial-related defects in diamond, Diam. Relat. Mater. 8 (8) (1999) 1560–1564.

[2] R. Kalish, A. Reznik, S. Prawer, D. Saada, J. Adler, Ion-implantation-induced defects in diamond and their annealing: Experiment and simulation, Phys. Status Solidi A 174 (1) (1999) 83–99.

[3] R. Kalish, A. Reznik, K.W. Nugent, S. Prawer, The nature of damage in ion-implanted and annealed diamond, Nucl. Instrum. Methods Phys. Res. B 148 (1) (1999) 626–633.

[4] H. Amekura, N. Kishimoto, Effects of high-fluence ion implantation on colorless diamond self-standing films, J. Appl. Phys. 104 (6) (2008) 63509.

[5] D.N. Jamieson, S. Prawer, K.W. Nugent, S.P. Dooley, Cross-sectional Raman microscopy of MeV implanted diamond, Phys. Rev. B 106 (1995) 641–645.

[6] J.H. Parker, D.W. Feldman, M. Ashkin, Raman scattering by silicon and germanium, Phys. Rev. 155 (1967) 712–714.

[7] M.W. Doherty, N.B. Manson, P. Delaney, F. Jelezko, J. Wrachtrupe, L.C. Hollenberg, The nitrogen-vacancy colour centre in diamond , Phys. Rep. 528 (2013) 1–45.

[8] A. Ferrari, S. Salustro, F. Gentile, W. Mackrodt, R. Dovesi, Substitutional nitrogen atom in diamond. a quantum mechanical investigation of the electronic and spectroscopic properties, Carbon 134 (2018) 354–365.

[9] A. Platonenko, F. Colasuonno, F.S. Gentile, F. Pascale, R. Dovesi, Oxygen and vacancy defects in silicon. A quantum mechanical characterization through the IR and Raman spectra, J. Chem. Phys. (2021).

[10] A. Ferrari, S. Salustro, F. Gentile, W. Mackrodt, R. Dovesi, Substitutional nitrogen atom in diamond. A quantum mechanical investigation of the electronic and spectroscopic properties, Carbon 134 (2018) 354–365.

[11] A. Platonenko, F.S. Gentile, F. Pascale, A.M. Ferrari, M. D'Amore, R. Dovesi, Nitrogen substitutional defects in silicon. A quantum mechanical investigation of the structural, electronic and vibrational properties, Phys. Chem. Chem. Phys. 21 (37) (2019) 20939–20950.

[12] A. Platonenko, F.S. Gentile, J. Maul, F. Pascale, E.A. Kotomin, R. Dovesi, Nitrogen interstitial defects in silicon. A quantum mechanical investigation of the structural, electronic and vibrational properties, Mat. Today Comm. 21 (2019) 100616.

[13] F. Gentile, A. Platonenko, K. El-Kelany, M. Rérat, P. D'arco, R. Dovesi, Substitutional carbon defects in silicon. A quantum mechanical characterization through the IR and Raman spectra, J. Comput. Chem. 41 (17) (2020) 1638—1644.

[14] A.D. Becke, Density-functional thermochemistry. III. The role of exact exchange, J. Chem. Phys. 98 (7) (1993) 5648–5652.

[15] C. Lee, W. Yang, R. Parr, Development of the colle-salvetti correlation-energy formula into a functional of the electron density, Phys. Rev. B 37 (2) (1988) 785–789.

[16] R. Dovesi, F. Pascale, B. Civalleri, K. Doll, N. Harrison, I. Bush, P. D'Arco, Y. Noël, M. Rérat, P. Carbonnière, M. Causà, S. Salustro, V. Lacivita, B. Kirtman, A. Ferrari, F. Gentile, J. Baima, M. Ferrero, R. Demichelis, M. De La Pierre, The CRYSTAL code, 1976–2020 and beyond, a long story, J. Chem. Phys. 152 (20) (2020) 204111.

[17] G.D. Watkins, J.W. Corbett, Defects in irradiated silicon. I. Electron spin resonance of the si-*A* center, Phys. Rev. 121 (1961) 1001–1014, URL https://link.aps.org/doi/10.1103/PhysRev.121.1001.